

# THE STUDIES OF OPTIMUM WAVELENGTH CHOICE IN DISTRIBUTED ROUGHNESS LAMINAR FLOW CONTROL TECHNIQUE

**Yueli Li, Dong Li, Yong Yang**

**National Key Laboratory of Science and Technology on Aerodynamic Design and  
Research, School of Aeronautics, Northwestern Polytechnical University, Xi'an, China**

*Keywords: Swept wing, Three-dimension Orr-Sommerfeld equation, Optimum control  
wavelength, Silk-screen, Transition delay.*

## Abstract

*The key technique of swept wing distributed roughness laminar flow control technique is how to confirm the cross-flow disturbance wavelength used to control transition. The optimum control wavelength of infinite swept wing is studied with the point of physical mechanism of control wave and flow interaction. The method to determine the wavelength is discussed in this paper. By using this method, 8mm is the optimum control wavelength under Saric's experimental condition which consists with Saric's experimental result. By using adaptive search method 1.72mm is obtained as the optimum control wavelength under NWPU model testing condition. By using silk-screen technique roughness array with roughness elements spacing of 1.7mm is added at leading-edge  $x/c=4\%$ , and transition location is delayed to trailing-edge.*

## 1 General Introduction

Drag reduction is one of the important objects in transport aircraft manufacturing, and delaying transition is viewed as the major solution to this problem. Series of experiments and computational investigation on transition to turbulence in cross flow dominated swept wing boundary layers conducted by Saric and his co-workers at AUS (Arizona State University) have indicated that: transition can be delayed effectually by leading-edge roughness array [1]. The approach referred to as the Distributed Roughness Technique. Compared with previous active control, passive laminar flow control has many advantages, therefore, further research

based on it [2] [3] [4]. Northwestern Polytechnical University (NWPU) is also engaging in the investigation at its low turbulence wind tunnel.

As the most widely used wing configuration in aircraft field, swept wing contains four types of instability mechanism [5] [6], which has been paid more attention to in both theory investigation and practical application. Researches have indicated that: cross-flow stationary wave plays a leading part in transition under low turbulence environment and favorable pressure gradients [2] [6]. In order to achieve stable cross flow stationary dominated experimental condition, Saric adopted NLF (2)-0415 airfoil beside low turbulence wind tunnel. As favorable pressure gradient can depress T-S mechanism and enhance instability of stationary wave, angles of attack from -4 degree to -2 degree were used to obtain ideal favorable pressure gradient [1][3][7], then they obtained most instable wavelength of 12 mm and control wavelength of 8mm as a result [1], which is the base of the followed investigations.

The traditional numerical investigation of Saric's experiment is that linear stability equation is usually used to calculate the most instable mode, then investigate the interaction under various initial conditions by using nonlinear PSE [3] [4]. However, the pivotal problem of this method is that besides the obtained data under Saric's experimental condition (most instable wavelength of 12 mm and control wavelength of 8 mm), there are no more detail about control wavelength [2]. This

will bring difficulties in numerical analysis when the condition varies.

In this paper, a new approach of optimum wavelength choice on the basis of understanding of passive laminar flow control physical mechanism has been presented. And an experiment has been designed to prove the feasibility of this theory qualitatively.

## 2 Control Wavelengths

Saric mentioned frequently in his paper [2] [6] that, since the stationary wave dominates transition progress on swept wing boundary layers, the key of passive laminar flow control mechanism is to artificially introduce short wavelength mode with quick amplification rate. Under Saric's experimental condition, the 8mm mode's amplification with fairly quick growth rate in early period, then immediately becomes saturated and finally decays. Taking use of it's nonlinearly interaction with other modes, and modifies mainstream velocity profile so as to depress the development of the most instability mode.

By authors' understanding, the disturbance wavelength that used for transition control of the flow on swept wing should has the quickest growth rate, which has the biggest slope in en curve.

Slope can be written as follow:

$$k = \frac{\partial n}{\partial x} \quad (1)$$

And the n factor formula is :

$$n = -\int_{x_0}^x \alpha_i dx \quad (2)$$

Then the slope can be equally transformed into the maximal growth rate of disturbance wavelength in linear theory:

$$k = -\alpha_i \quad (3)$$

So, the expression can be written as:

$$\beta_r |_{\max(k)} = \beta_r |_{\max(\alpha_i)} \quad (4)$$

Non-dimensional span-wise wave number expressed in  $\beta_r$ .

Disturbance wave at a certain wave band may develop into the most instable wave and finally brings forth transition, which is related to receptivity mechanism. Instable mode can only be detected at 10% relative chord length position in Saric's experiment [1]. That's to say, control wavelength should quickly modifies the main flow velocity profile which is suitable to the most instable disturbance development before 10% relative chord length, so that the most instability disturbance's amplification may be depressed, and transition will be delayed.

So the formula 4 can further into:

$$\beta_r |_{\max(k)} = \beta_r |_{\max(\alpha_i)} \quad (x/C \leq 10\%) \quad (5)$$

Although linear instability equation is unable to analyze the detailed interaction among modes, it can find out which has the quickest growth rate among all the wavelengths. Therefore, wavelength range used for the proper control can be easily found out. In this paper, investigation followed the idea that the wavelength with the quickest grow rate can be obtained through calculating 3D incompressible linear stability equation (without curvature effect) on the basis of incompressible flow filed data has been done.

## 3 Numerical calculations

### 3.1 Flow field calculation

Three-dimensional swept wing boundary velocity profile is calculated by using IBL2D [8] and BLISW [9] both of which coded by Cebeci. The authors configure pre- and post-process codes for them.

### 3.2 Stability characteristics calculation

The three-dimension swept wing boundary layer dynamic instability characteristics are obtained by calculating three-dimension incompressible linear stability equations by using LST3DM01 (Linear Stability Theory 3D Mack 01) and LST3DM02 (Linear Stability Theory 3D Mack 02). They are three-dimension linear instability equation Mack's method codes coded by Li Yue-Li. LST3DM01

is a fixed mode calculation program, which can get modes' n factor and its growth rate. LST3DM02 is an adaptive search calculation code, which can find out the optimum mode. Calculation start from 5% relative chord length [5] [10], and end at pressure minimum station supplied by IBL2D.

#### 4 Calculation and analyze

To validate the previous assumption that the optimal laminar flow control wavelength has the quickest growth rate, two examples are investigated as follows. One is the Saric's model; the other is present experiment in NWPU:

Table.1 calculation conditions

	Baseline(Saric)	Extraline(NWPU)
Aerofoil	NLF(2)-0415	NLF(2)-0415
chord	1.83m	0.4m
Swept angle	45 degree	45 degree
Reynolds	2400000	2200000
Attack angle	-4.0	-4.0
Mach	0.0563	0.2361
Velocity	19.1570 m/s	80.0 m/s

On baseline analyze, [6, 8, 9, 12, 15, 18, 24, 36] mm span-wise wavelengths are chosen as the introduced disturbances, the en curves are calculated by using LST3DM01. Fig.1 shows that 8mm's growth rate is a maximum one among the wavelengths before  $x/c=10\%$ , it can be used as the control wavelength, and authors' previous assumption has been conformed. On the extra-line analyze, from LST3DM02 code, we can find the growth rate of 1.72mm is maximum as Fig.2 illustration, and we chose

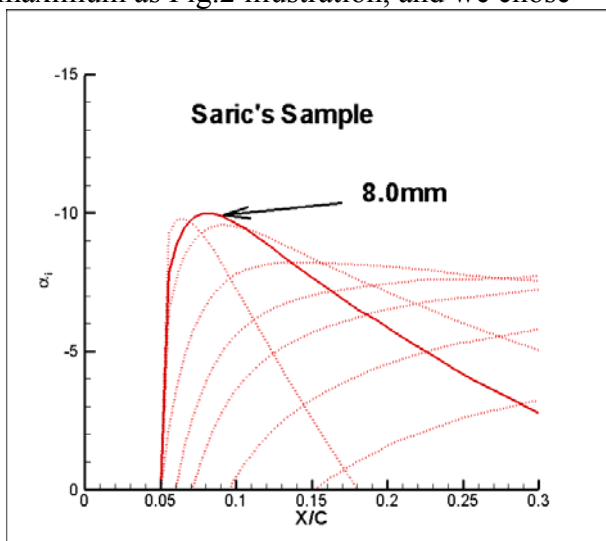


Fig.1. Baseline growth rate curve

1.7mm as a control mode under Extraline condition.

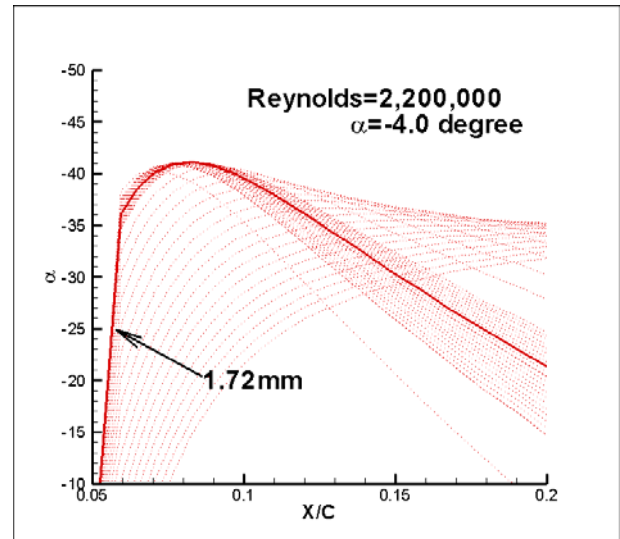


Fig.2. Extraline growth rate curve

#### 5 Experimental validated

To validate the numerical calculation result above further, an experiment has been carried out under Extraline condition. Experiment is conducted at NWPU's NF-3 wind tunnel. The turbulence level is  $Tu=0.00035$ , which is beyond  $Tu=0.0015$  [7], and suits to cross-flow dominated transition experiment. The model has a NLF (2)-0415 profile, a 0.4m un-swept chord length, with 45 degree swept, and its surface natural roughness is  $0.4\mu\text{m}$ . The model is mounted in wind tunnel at -4 degree attack angle as Fig.3 shows. Silk-screen technique is used to add roughness elements on the surface of the model to meet the requirement of roughness element spacing precision. Roughness height depends on silk-screen rubber thickness,  $10\mu\text{m}$  rubber is employed. Each roughness element is a hemisphere whose diameter is 0.4mm, and the interval between two centers of elements is 1.7mm. The roughness array is located at 4% relative chord. Fig.4 is silk-screen sketch map. Fig.5 and Fig.6 show the detail of roughness elements and roughness array especially.



Fig.3. Model mounted in wind tunnel

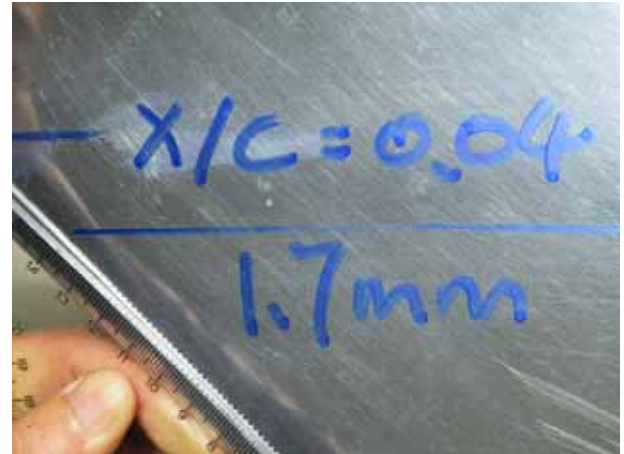


Fig.6. Roughness array detail

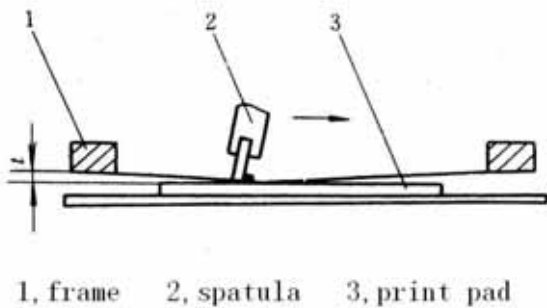


Fig.4. Silk-screen sketch map



Fig.5. Roughness element detail

Transition location is visualized by sublimation method in this paper; naphthalene is used as indicator and acetone as solvent. Experiment is divided into two groups, one is natural roughness, the other is with roughness array which roughness elements interval is 1.7mm located at  $x/c=4\%$ . In order to avoid the bypass transition caused by crystallization particles during the spraying process as Fig.7 shows, leading-edge is not sprayed before  $x/c=30\%$  as Fig.8 presents.



Fig.7. Bypass transition



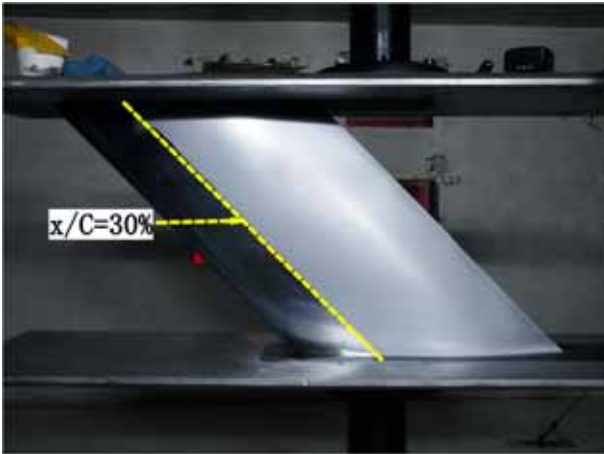


Fig. 8. Leading-edge unsprayed until  $x/c=30\%$

Wind tunnel experimental condition is consistent with the Extraline condition. As Fig.9 shows, when model without roughness, saw-tooth shape appears at  $x/c=50\%$ , and extend to  $x/c=70\%$ . Saw-tooth shape transition phenomena can be judged as cross-flow stationary wave dominated transition [11]. Fig.10 is with roughness array experimental result, as it shows, although saw-tooth shape appears at  $x/c=50\%$ , its intensity is not strong enough to trigger transition in downstream pressing, and transition has been delayed to  $x/c=100\%$  finally.

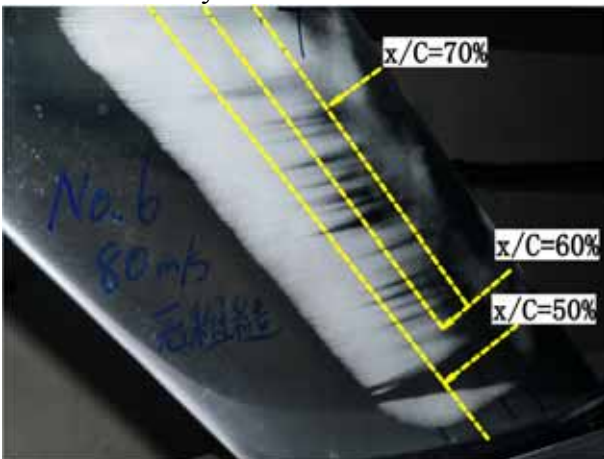


Fig.9. Experimental result, without roughness

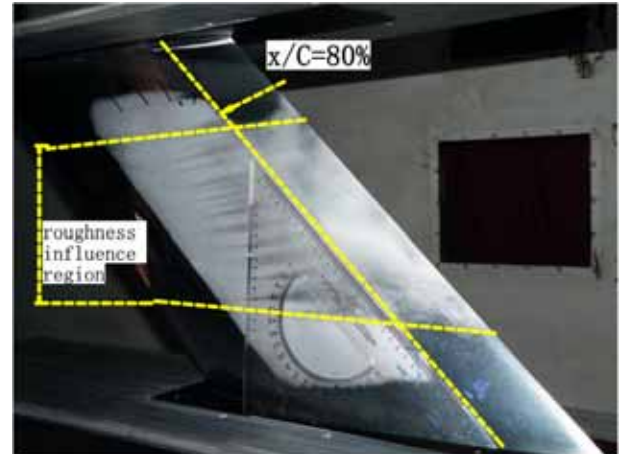


Fig.10. Experimental result, with roughness

## 6 Discussions

Roughness array parameters include elements' interval, array's location, element's height and element's diameter. Elements' interval comes from calculation that based on previous assumption. It can be defined accurately by LST3DM02 calculation at the very start while the flow condition has been altered. Roughness elements' height and location are mutually linked, and associates with receptivity mechanism. Unfortunately, detailed physical receptivity mechanisms for cross flow have not been investigated experimentally. In this paper, numerical computation and experiment show that, disturbance introduced position will not influence its control mode's characteristics but impact on its  $n$  factor, that is to say roughness array location will influence the magnitude of disturbance distort main flow only. Growth rate calculation as Fig.11 shows that the location variety only shifts the maximum of  $\alpha_i$ , but its location. As Fig.12 shows,  $n$  factor curves are approximate parallel. The optimum control wavelength can be calculated by LST3DM02, but the optimum initial amplitude is difficulty to determine. So, when roughness height has been fixed on, shifts roughness location around  $x/c=5\%$  will be able to change the initial amplitude. And then find out the optimum initial amplitude to delay the transition. Roughness elements diameter chosen should consider two restrictions. One is the instinct of silk-screen technique. Diameter should be not too small; or it may impact the

effect of handmade printing. Another is for the interval. Diameter should not be too big, or it will influence the expression of introduced stationary wavelength. So, 0.4mm is the Optimum diameter under interval under 1.7mm condition.

Although an experiment has been conducted to validate the previous assumption, more detail data of velocity profiled are still void. This is due to the instinct of receptivity mechanism. In Saric's experiments, velocity profiled measured by hot wire beyond  $x/c=0.3$ . The more forward, the more risk of trigger bypass transition; and then destroy flow field character. And more, PIV technique may have this problem.

That is why the upper surface of the model is not sprayed before  $x/c=30\%$ . Velocity profiled measured data beyond  $x/c=0.3$  only validates the most instability mode be depressed, But, by reason of control mode modifies the main flow at its early evolution stage.

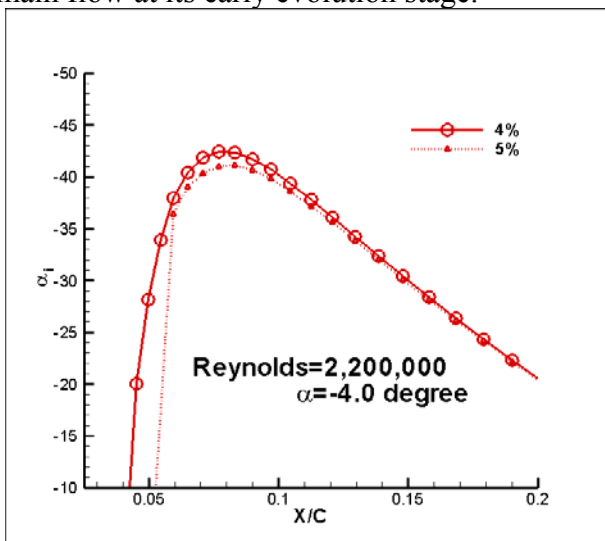


Fig.11. Growth rate curve

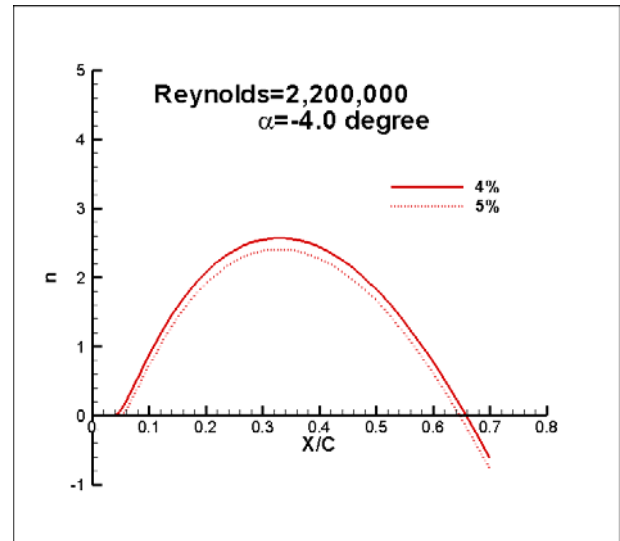


Fig.12. n factor curve

## 7 Conclusions

Basis on eq.5 [6, 8, 9, 12, 15, 18, 24, 36]mm disturbance wavelength have been analyzed under baseline by using LST3DM01, numerical calculation result has confirm that, growth rate of 8mm wavelength is the maximum before 10% relative chord length, and 8mm the practical control wavelength under baseline condition. This calculation result is consists with Saric's experimental result. And then, by using LST3DM02, the control wavelength under extra-line is found to be 1.72mm. Experiment has been designed to validate the numerical calculation at NWPU's NF-3 wind tunnel. Without leading-edge roughness array, the swept wing's transition location begin at  $x/c=50\%$ , and completely transition at  $x/c=70\%$ . After the 1.7mm spacing roughness array is set on leading-edge at  $x/c=4\%$ , transition location has been delayed to  $x/c=100\%$ . The previous assumption and numerical calculation have been confirmed.

Silk-screen technique could improve the roughness element spacing precision, and suits for micro-meter level roughness element height control. Roughness elements location shifts in stream wise will not influence mode's characteristics, but proper shift could help achieving the optimum initial amplitude and actualize transition delay.

## **References**

- [1] William S. Saric, Ruben B. Carrillo, Jr. and Mark S. Reibert. Leading-Edge Roughness as a Transition Control Mechanism. AIAA-98-0781.
- [2] William S. Saric and Helen L. Supersonic laminar flow control on swept wings using distributed roughness. AIAA 2002-0147.
- [3] C. J. Atkin and M. S .Mughal. Parametric PSE Studies on Distributed Roughness Laminar Flow Control. AIAA 2006-3694.
- [4] C. J. Atkin and M. S .Mughal. Parametric Studies on the Application of Distributed Roughness Elements for Laminar Flow Control. AIAA 2005-5263.
- [5] William S. Saric and Helen L. Reed. Toward Practical Laminar Flow Control—Remaining Challenges. AIAA 2004-2311.
- [6] William S. Saric and Helen L. Reed. Crossflow instabilities-theory & technology. AIAA-03-0771.
- [7] E.B. White, W.S. Saric, R.D. Gladden and P.M. Gabet. Stages of Swept-Wing Transition. AIAA-01-0271
- [8] Tuncer Cebeci. *Stability and Transition: Theory and Application*. Long Beach, Calif.: Horizons Pub, pp 85-111, 2004.
- [9] Tuncer Cebeci. *Stability and Transition: Theory and Application*. Long Beach, Calif.: Horizons Pub, pp114-148, 2004.
- [10] Tuncer Cebeci. *Modeling and Computation of Boundary-Layer Flows*. Horizons Publishing Inc. Long Beach, pp262-263, 2005.
- [11] Mark S. Reibert and William S. Saric. Review of Swept-Wing Transition. AIAA-1997-1816.

## **Copyright Statement**

The authors confirm that they, and/or their company or organization, hold copyright on all of the original material included in this paper. The authors also confirm that they have obtained permission, from the copyright holder of any third party material included in this paper, to publish it as part of their paper. The authors confirm that they give permission, or have obtained permission from the copyright holder of this paper, for the publication and distribution of this paper as part of the ICAS2010 proceedings or as individual off-prints from the proceedings.